

Role of structural defects in the unipolar resistive switching characteristics of Pt/NiO/Pt structures

Chanwoo Park,¹ Sang Ho Jeon,² Seung Chul Chae,³ Seungwu Han,⁴ Bae Ho Park,² Sunae Seo,⁵ and Dong-Wook Kim^{4,a)}

¹Department of Applied Physics, Hanyang University, Ansan, Gyeonggi-do 426-791, Republic of Korea

²Department of Physics, Konkuk University, Seoul 143-701, Republic of Korea

³Department of Physics and Astronomy, Seoul National University, Seoul 151-747, Republic of Korea

⁴Department of Physics, Ewha Womans University, Seoul 120-750, Republic of Korea

⁵Samsung Advanced Institute of Technology, Suwon, Gyeonggi-do 440-600, Republic of Korea

(Received 20 May 2008; accepted 2 July 2008; published online 28 July 2008)

We investigated the resistive switching characteristics of two types of Pt/NiO/Pt structures with epitaxial and polycrystalline NiO layers. Both of these Pt/NiO/Pt structures exhibited unipolar resistive switching. Pt/epitaxial-NiO/Pt showed unstable switching or no resistance state change after several repeated runs. Pt/polycrystalline-NiO/Pt showed very reproducible switching. The experimental data indicated that microstructural defects (e.g., grain boundaries) played crucial roles in the reliability of the unipolar resistive switching behavior. This was further supported by first-principles calculations. © 2008 American Institute of Physics. [DOI: 10.1063/1.2963983]

Resistive switching (RS) in metal/oxide/metal (MOM) structures requires either polarity reversal (bipolar RS) or magnitude variation (unipolar RS) of the applied bias voltage.¹⁻¹⁰ The conducting filament formation and rupture model well describe the unipolar RS characteristics.²⁻⁸ However, the mechanism responsible for bistable resistance states is still controversial. Polycrystalline thin films have been reported to show both bipolar and unipolar RS,²⁻⁹ while most epitaxial thin films exhibit bipolar RS.^{2,10} These observations suggest that the dominant RS mechanism may depend not only on the material but also on its crystalline form.² The use of different bottom electrode materials allows control of the structural quality of MOM structures.¹⁰ However, electrode materials can alter the defect concentration as well as the electronic and chemical interactions at the metal-oxide interface.^{9,10} It is desirable to control the structural quality of MOM structures with identical constituent materials to understand the role of crystalline disorder in RS.

We investigated the influence of structural defects on the electrical properties and RS behaviors of Pt/NiO/Pt structures. Both epitaxial and polycrystalline NiO thin films showed unipolar RS. The polycrystalline samples exhibited more reliable switching than the epitaxial samples. Based on first-principles calculations, we suggest a possible explanation for the RS mechanism.

We prepared thermally oxidized NiO thin films on Pt bottom electrodes grown on two kinds of substrates: single-crystal sapphire (Al₂O₃) and silicon with thermal oxide (SiO₂/Si).⁸ We analyzed the crystalline quality of the thin films by high-resolution x-ray diffraction (XRD). To characterize the electrical properties, we deposited the 30 nm Au/10 nm Pt top electrode layers with a shadow mask (area: 46 × 46 μm²) using an e-beam evaporator. All of the electrical measurements were obtained using a probe station and an HP 4145B semiconductor parameter analyzer at room temperature.

Figures 1(a) and 1(b) show typical XRD θ - 2θ scan and ϕ -scan results of a 60-nm-thick NiO/200 nm Pt layer grown on a Al₂O₃(0001) substrate. The peak at $2\theta=37.3^\circ$ corresponds to the NiO(111) plane reflection, indicating a single-phase NiO film formed with the preferred crystalline axis. The ϕ -scan results around the NiO(200) and Pt(200) peaks show six distinct peaks with 60° separations, indicating the epitaxial relationship of NiO[100]||Pt[100]. The ϕ -scan measurements around the Al₂O₃[1014] peaks (data not shown) confirmed the epitaxial growth of Pt[110]||Al₂O₃[1010] structure, as reported previously.¹¹ The XRD analyses of NiO/Pt/TiO_x/SiO₂/Si thin films (TiO_x layers inserted as adhesion layers) revealed that the in-plane crystalline axes of the NiO and Pt grains were randomly distributed and contained large-angle grain boundaries. Hereafter, the Pt/NiO/Pt/Al₂O₃ and Pt/NiO/Pt/TiO_x/SiO₂/Si structures will be referred to as Pt/epi-NiO/Pt and Pt/poly-NiO/Pt, respectively.

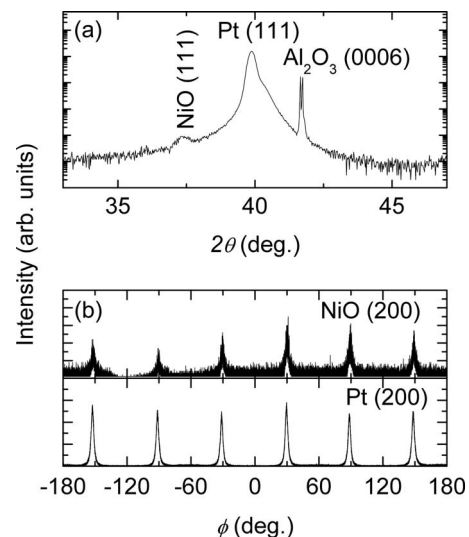


FIG. 1. (a) XRD θ - 2θ scan result of a NiO film grown on a Pt(111)||Al₂O₃(0001) substrate and (b) ϕ -scan plot of Ni(200) and Pt(200) reflections.

^{a)}Electronic mail: dwkim@ewha.ac.kr.

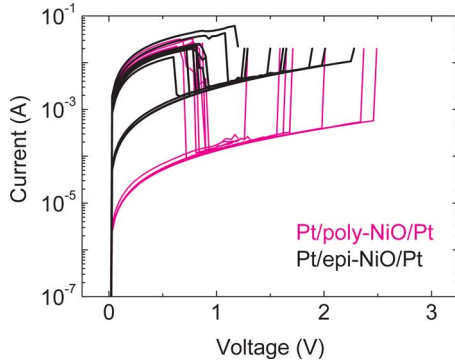


FIG. 2. (Color online) Typical I - V characteristics of Pt/NiO/Pt/ $\text{TiO}_x/\text{SiO}_2/\text{Si}$ and Pt/NiO/Pt/ Al_2O_3 obtained during repetitive switching cycles.

We performed dc-voltage sweep measurements for Pt/epi-NiO/Pt and Pt/poly-NiO/Pt in the temperature (T) range from 20 to 200 °C (data not shown). All of the current-voltage (I - V) curves were symmetrical, and the current for the initial state (I_i) was greater at higher measurement temperatures. Curves of $\ln(I_i)$ versus $1/k_B T$ showed linear behavior, which indicates that both of our epitaxial and polycrystalline NiO thin films follow the correlated polaron hopping model.⁶ Estimated thermal activation energy (φ_i) values of the Pt/epi-NiO/Pt and Pt/poly-NiO/Pt structures were similar and ranged from 200 to 300 meV, comparable to those in previous reports.⁶ Conduction through the large-angle grain boundaries, for the polycrystalline film, does not dominate the transport.

Figure 2 shows typical I - V curves of Pt/epi-NiO/Pt and Pt/poly-NiO/Pt during repeated switching cycles. During the high-to-low resistance switching (set) process, we limit the current to 20 mA to avoid permanent damage to the samples.⁸ Both of the Pt/NiO/Pt structures exhibit repetitive RS in the unipolar mode. Lee *et al.* reported that epitaxial NiO thin films, grown on the SrRuO₃ bottom electrodes, showed bipolar RS.¹⁰ The use of different bottom electrode materials, Pt and SrRuO₃, alters the RS mode and highlights the importance of interfacial effects in the RS behaviors of MOM structures.^{4,5}

The high-resistance-state (HRS) resistance of Pt/epi-NiO/Pt is two orders of magnitude smaller than that of Pt/poly-NiO/Pt. Since the HRS conduction follows the polaron hopping model at around room temperature,⁶ the two kinds of NiO samples seem to have different mobilities and/or carrier densities. In contrast, low-resistance-state current levels of Pt/epi-NiO/Pt are not largely different from those of Pt/poly-NiO/Pt. This suggests that the conducting filaments formed in both epitaxial and polycrystalline NiO thin films have similar behaviors.

As shown in Fig. 2, the set voltage (V_{set}) and the low-to-high-resistance switching (reset) voltage (V_{reset}) vary significantly, possibly related to the percolative nature of RS.³ Note that V_{reset} for Pt/epi-NiO/Pt has a wider distribution than that for Pt/poly-NiO/Pt. An additional difference was clear in the switching yield, i.e., number of pads showing reproducible RS/number of pads tested. For Pt/poly-NiO/Pt, 11 of 12 pads showed reproducible RS behavior. In contrast, only 8 of 17 pads for Pt/epi-NiO/Pt showed repetitive RS. For the RS-failed pads, we did not observe reset, even with application of a sweeping bias voltage of up to 2.0 V, which

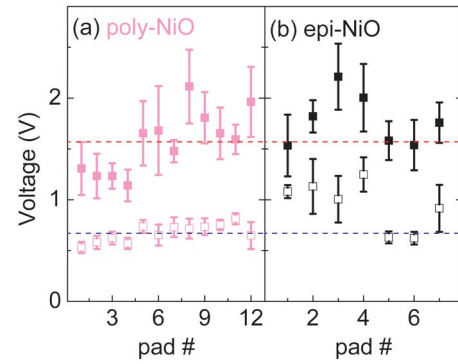


FIG. 3. (Color online) Switching voltage distribution of pads (obtained during ten switching cycles) in (a) Pt/NiO/Pt/ $\text{TiO}_x/\text{SiO}_2/\text{Si}$ (polycrystalline NiO) and (b) Pt/NiO/Pt/ Al_2O_3 (epitaxial NiO). Filled and open squares indicate set and reset voltages, respectively. Dotted lines correspond to average set and reset voltages for the polycrystalline NiO sample.

was well over the mean value of V_{set} (1.67 V) for Pt/epi-NiO/Pt. Figures 3(a) and 3(b) clearly show the switching voltage distribution [10 set/reset cycles for each pad] from Pt/poly-NiO/Pt (12 pads) and Pt/epi-NiO/Pt (eight pads), respectively. Difference in the average values of V_{reset} (Pt/epi-NiO/Pt: 0.88 V, Pt/poly-NiO/Pt: 0.67 V) is notable compared with those of V_{set} (Pt/epi-NiO/Pt: 1.67 V, Pt/poly-NiO/Pt: 1.57 V). The crystalline quality of the NiO layers affects the RESET process to a greater extent than the SET process.

We performed first-principles calculations to investigate the role of the grain boundaries, based on the computational setup described previously.¹² Figure 4(a) shows a model

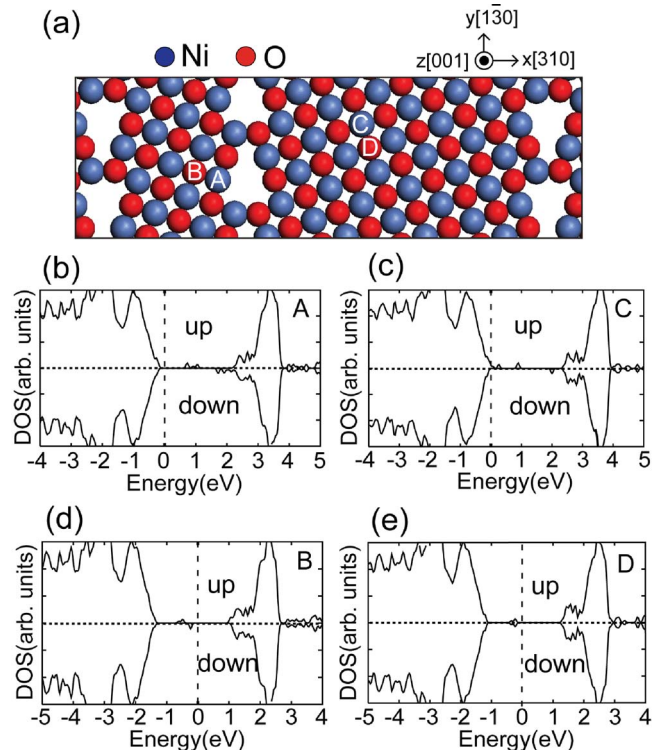


FIG. 4. (Color online) (a) Model structure for $\Sigma 5(310)[001]$ grain boundary in NiO. The vacancy sites are marked by A–D. [(b) and (c)] The spin-decomposed DOS for nickel vacancies at sites A and C in (a), respectively. [(d) and (e)] DOS for oxygen vacancies at sites B and D in (a), respectively. The Fermi level is set to zero.

structure of the $\Sigma 5(310)[001]$ tilt grain boundary of NiO. We estimated the formation energies of nickel and oxygen vacancies at various positions in Fig. 4(a), and the formation energies were lower at the grain boundary by approximately 0.4–0.6 eV and 0.1–0.2 eV for nickel and oxygen vacancies, respectively. As expected, the vacancies may exist predominantly near the grain boundaries.⁵ To investigate the electronic structures, we plot the density of states (DOS) when the vacancies are at the grain boundary or in the bulk [Figs. 4(b)–4(e)]. The DOS for the vacancies in the bulk region shows good agreement with the results reported previously.¹² Interestingly, the nickel vacancies at the grain boundary do not generate hole carriers [Fig. 4(b)], in contrast to the bulk case where the partially occupied valence top led to *p*-type conductivity [Fig. 4(c)].¹² These results indicate that grain boundaries with large defect concentrations are not necessarily conducting, which is somewhat contrary to intuitive expectations. Our experimental data support the calculation results; the initial state and HRS resistance of Pt/poly-NiO/Pt is higher than that of Pt/epi-NiO/Pt. It is noted that since the grain boundary mostly affects the conduction part of DOS, it is likely that the foregoing observations are not affected much by the orientation of the grain boundary.

Previous studies revealed that the SET process resembles the soft breakdown of a dielectric layer and results in the formation of a percolative network of conducting paths, so-called filaments.^{3–8} Temperature-dependent transport measurements suggested that the filaments in NiO may consist of metallic Ni defects.⁶ This implies that the subsequent reset process is equivalent to filament reoxidation through the migration of ions. During reset, Joule heating caused by the localized current distribution along the filamentary paths can enhance ion migration and oxidation.^{7,8}

We estimated the migration barrier for the oxygen vacancies, which could be related to the reset voltages. In the case of bulk NiO, the migration barrier is 2.3 eV for doubly ionized oxygen vacancies. The calculation of the barrier for the grain boundary is beyond our computational capabilities. Instead, we considered the migration of oxygen vacancies on the surface. It was found that the barrier was significantly lowered to 1.2 eV. Due to the empty space above the surface, oxygen atoms can relax the strained Ni–O bonds during migration by protruding from the surface. A similar effect

should apply to the grain boundary albeit to a lesser extent. The migration of oxygen vacancies or atoms is facilitated along the grain boundary, which therefore explains the low switching voltage for polycrystalline samples.

In summary, we investigated unipolar RS behaviors of Pt/NiO/Pt structures with epitaxial and polycrystalline NiO layers. The epitaxial NiO layer showed a large voltage variation for low-to-high-resistance state switching and poor reproducibility during repeated switching cycles. First-principles calculation suggested that the low migration energy at the grain boundary helped to create reliable switching. This result emphasized the importance of crystalline defects in the RS phenomena of MOM structures.

This work was supported by the Korea Research Foundation Grant funded by the Korean Government (MOEHRD) (KRF-2007-331-C00083). S.H. and B.H.P. were supported by the National Program for 0.1 Terabit NVM Devices. B.H.P. was also supported by the KOSEF NRL Program grant funded by the Korea government (MEST) (No. R0A-2008-000-20052-0).

¹M.-J. Lee, Y. Park, D.-S. Suh, E.-H. Lee, S. Seo, D.-C. Kim, R. Jung, B.-S. Kang, S.-E. Ahn, C. B. Lee, D. H. Seo, Y.-K. Cha, I.-K. Yoo, J.-S. Kim, and B. H. Park, *Adv. Mater. (Weinheim, Ger.)* **19**, 3919 (2007).

²R. Waser and M. Aono, *Nat. Mater.* **6**, 833 (2007).

³S. C. Chae, J. S. Lee, S. Kim, S. B. Lee, S. H. Chang, C. Liu, B. Kahng, H. Shin, D.-W. Kim, C. U. Jung, S. Seo, M.-J. Lee, and T. W. Noh, *Adv. Mater. (Weinheim, Ger.)* **20**, 1154 (2008).

⁴K. M. Kim, B. J. Choi, and C. S. Hwang, *Appl. Phys. Lett.* **90**, 242906 (2007).

⁵G.-S. Park, X.-S. Li, D. C. Kim, R. Jung, M.-J. Lee, and S. Seo, *Appl. Phys. Lett.* **91**, 222103 (2007).

⁶K. Jung, H. Seo, Y. Kim, H. Im, J. P. Hong, J.-W. Park, and J.-K. Lee, *Appl. Phys. Lett.* **90**, 052104 (2007).

⁷H. Shima, F. Takano, H. Akinaga, Y. Tamai, I. H. Inoue, and H. Takagi, *Appl. Phys. Lett.* **91**, 012901 (2007).

⁸D.-W. Kim, R. Jung, B. H. Park, X.-S. Li, C. Park, S. Shin, D.-C. Kim, C. W. Lee, and S. Seo, *Jpn. J. Appl. Phys.* **47**, 1635 (2008).

⁹T. Tsunoda, Y. Fukuzumi, J. R. Jameson, Z. Wang, P. B. Griffin, and Y. Nishi, *Appl. Phys. Lett.* **90**, 113501 (2007).

¹⁰S. R. Lee, K. Char, D. C. Kim, R. Jung, S. Seo, X. S. Li, G.-S. Park, and I. K. Yoo, *Appl. Phys. Lett.* **91**, 202115 (2007).

¹¹D. Lee, J.-H. Lee, S. Y. Jang, P. Murugavel, Y.-D. Ko, and J.-S. Chung, *J. Cryst. Growth* **310**, 829 (2008).

¹²S. Park, H.-S. Ahn, C.-K. Lee, H. Kim, H. Jin, H.-S. Lee, S. Seo, J. Yu, and S. Han, *Phys. Rev. B* **77**, 134103 (2008).